

Electronic Supplementary Information (ESI)

Silver-frameworks based on tetraphenylethylene-imidazole ligand for electrocatalytic reduction of CO₂ to CO

Yu-Jie Wang, Zhao-Feng Qiu, Ya Zhang, Fang-Fang Wang, Yue Zhao and Wei-Yin Sun*

Coordination Chemistry Institute, State Key Laboratory of Coordination Chemistry, School of Chemistry and Chemical Engineering, Nanjing National Laboratory of Microstructures, Collaborative Innovation Center of Advanced Microstructures, Nanjing University, Nanjing 210023, China

Email address: sunwy@nju.edu.cn (W.Y. Sun)

Materials and characterizations

The reagents used in the experiment were purchased and used directly without any post-treatment and purification. Silver nitrate (AgNO₃), 4,4'-oxybisbenzoic acid (H₂OBA), silver trifluoromethanesulfonate (AgCF₃SO₃) and potassium hydroxide (KOH) were purchased from Shanghai Titan Science Co., Ltd. Nafion reagent (5 wt%) was purchased from Sign Aldrich. Acetonitrile and isopropanol were purchased from China National Pharmaceutical Group Chemical Reagent Co., Ltd. 1,1,2,2-Tetrakis(4-(imidazol-1-yl)phenyl)ethene (TIPE) was synthesized according to the literature procedure.¹ Water used in the material preparation process is deionized water (18.25 Ω).

Powder X-ray diffraction patterns (PXRD) of the samples were measured on the Bruker D8 Advance X-ray diffractometer using Cu-Kα ($\lambda = 1.5418 \text{ \AA}$) radiation. During the testing process, the voltage of the instrument was 40 kV, the current was 40 mA. The total reflection infrared (ATR-IR) spectra of the samples were measured on the Fourier transform infrared (FT-

IR) spectrometer TENSOR 27 with a spectral range of 4000-400 cm^{-1} . TG data of the samples were obtained through testing on a Mettler-Toledo (TGA/DSC1) thermal analyzer, and thermogravimetric analysis was performed under nitrogen atmosphere at a heating rate of 10 $^{\circ}\text{C min}^{-1}$. Elemental content of the samples was determined by Elementar UNICUBE element analyzer. Transmission electron microscopy (TEM) images were obtained on JEOL-2010. Cyclic voltammetry (CV) profiles and electrochemical impedance spectroscopy (EIS) were performed on the Zahner electrochemical workstation (IM6ex, Zahner Scientific Instruments, German).

X-ray crystallography

Crystallographic data of the samples were collected on the Bruker D8 Venture and the Bruker smart apex II CCD area detector diffractometer. ϕ/ω scanning was performed with graphite monochromators Ga-K α ($\lambda = 1.34133\text{ \AA}$) and Mo-K α ($\lambda = 0.71073\text{ \AA}$), and the crystals were maintained at 193 K during data collection. The structures were solved by direct methods with SHELXT-2014, expanded by subsequent Fourier-difference synthesis, and all the non-hydrogen atoms were refined anisotropically on F^2 using the full-matrix least-squares technique using the SHELXL-2018 crystallographic software package. The details of crystal parameters, data collection and refinements for **Ag-MOF1** and **Ag-MOF2** are listed in Table 1, and the selected bond lengths and angles are given in Table S1.

Product quantification

The possible gas products (H_2 , CO , CH_4 , C_2H_4) were directly vented into the gas chromatograph system (GC 9790II, Fuli) equipped with a thermal conductivity detector (TCD) and a flame ionization detector (FID) with a methanizer. The possible liquid products were quantified by ^1H NMR spectroscopy (Bruker-DRX 500 MHz) using dimethyl sulfoxide (DMSO) as an internal standard. The pre-saturation method was used to suppress the water peak.

The FE was calculated using the following equations:

$$FE_{\text{gas}} = \frac{n \times F \times p \times V_{\text{gas}} \times q_{\text{gas}}}{i \times R \times T} \times 100\%$$

where n is the number of transferred electrons for products, $p = 101.3$ kPa, V_{gas} is the concentration of gas product detected by GC, F is the Faraday constant, $T = 298.15$ K, q_{gas} is the gas flow rate (20 mL min^{-1}), R is the gas constant, i is the total current density.

Table S1. Selected bond lengths (Å) and angles (°) for **Ag-MOF1** and **Ag-MOF2**.

Ag-MOF1			
Ag(1)-O(1)	2.5898(14)	Ag(1)-N(1)	2.314(9)
Ag(1)-N(1)#1	2.314(9)	Ag(1)-N(1)#2	2.314(9)
O(1)-Ag(1)-N(1)#1	112.1(2)	O(1)-Ag(1)-N(1)#2	112.1(2)
O(1)-Ag(1)-N(1)	112.1(2)	N(1)#1-Ag(1)-N(1)#2	106.8(2)
N(1)#1-Ag(1)-N(1)	106.8(2)	N(1)-Ag(1)-N(1)#2	106.8(2)
Ag(1)-O(1)-Ag(1)#3	109.5	Ag(1)-O(1)-Ag(1)#4	109.5
Ag(1)#4-O(1)-Ag(1)#3	109.5	Ag(1)#5-O(1)-Ag(1)#3	109.5
Ag(1)-O(1)-Ag(1)#5	109.471(1)	Ag(1)#4-O(1)-Ag(1)#5	109.471(1)
C(1)-N(1)-Ag(1)	130.5(7)	C(3)-N(1)-Ag(1)	120.1(7)

Symmetry transformations used to generate equivalent atoms: #1 1-Y,1-Z,+X;

#2 +Y,1-Z,1-X; #3 +Y,1-Z,1-X; #4 1-Z,+X,1-Y; #5 1-Y,1-X,+Z;

Ag-MOF2			
Ag(1)-N(1)#1	2.119(5)	N(1)-Ag(1)-N(1)#1	180.0
C(1)-N(1)-Ag(1)	126.2(4)		

Symmetry transformations used to generate equivalent atoms: #1 3/2-X,3/2-Y,1-Z;

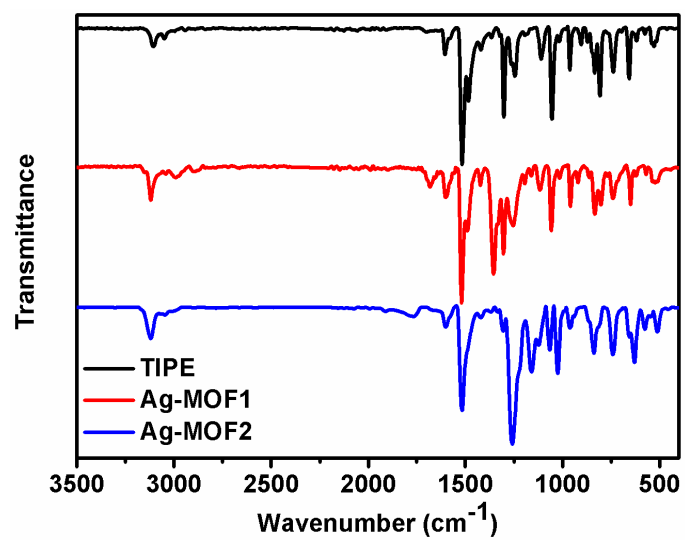


Fig. S1 FT-IR spectra of TIPE, Ag-MOF1 and Ag-MOF2.

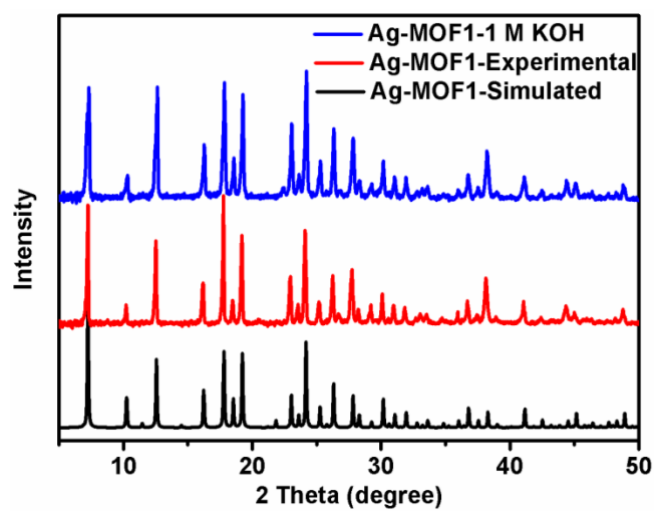


Fig. S2 PXRD patterns of Ag-MOF1.

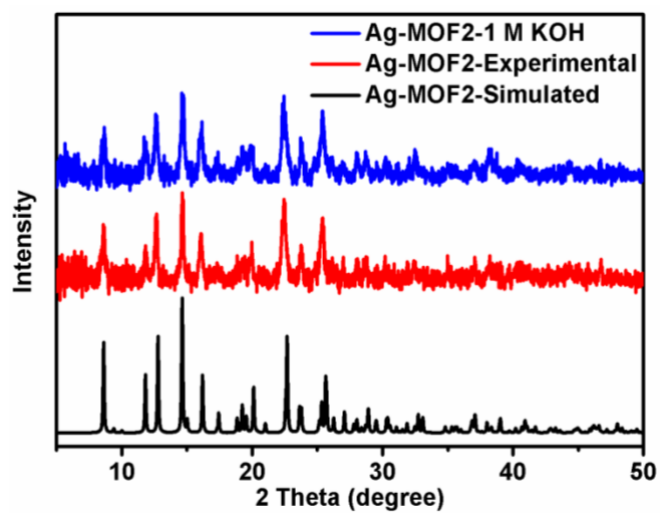


Fig. S3 PXR D patterns of Ag-MOF2.

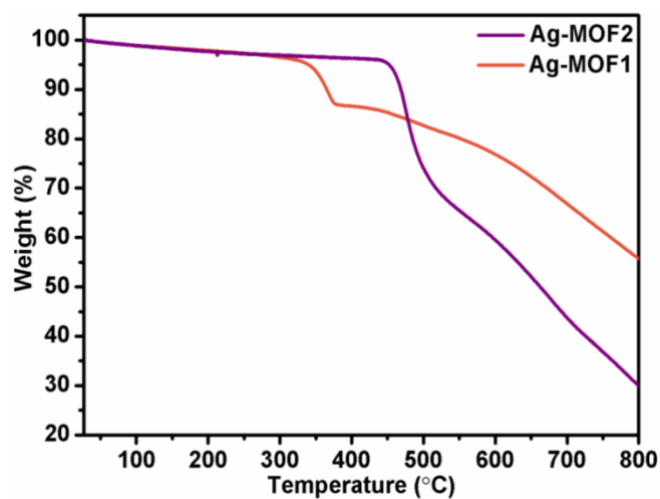


Fig. S4 TG curves of Ag-MOF1 and Ag-MOF2.

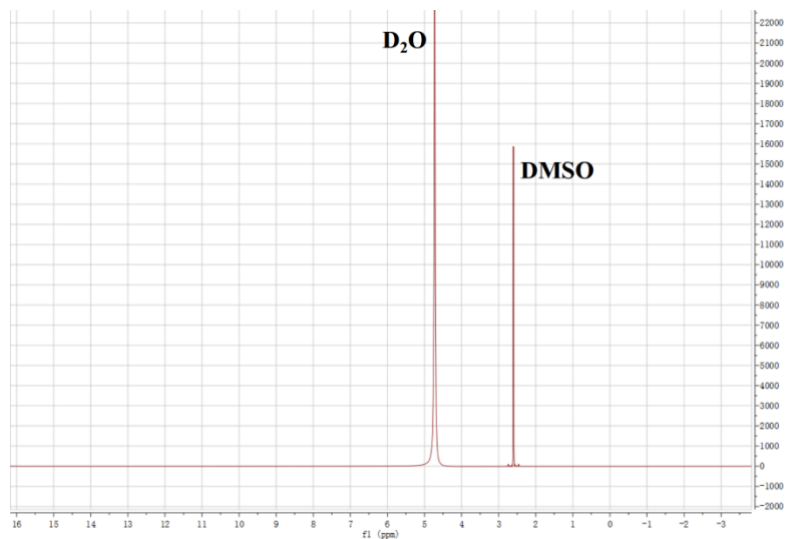


Fig. S5 ^1H NMR spectrum of electrolyte after CO_2RR .

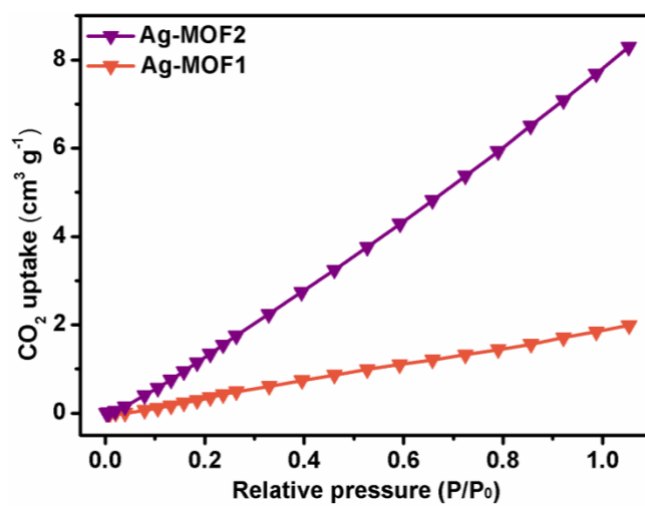


Fig. S6 CO_2 adsorption isotherms of Ag-MOF1 and Ag-MOF2 at 273 K.

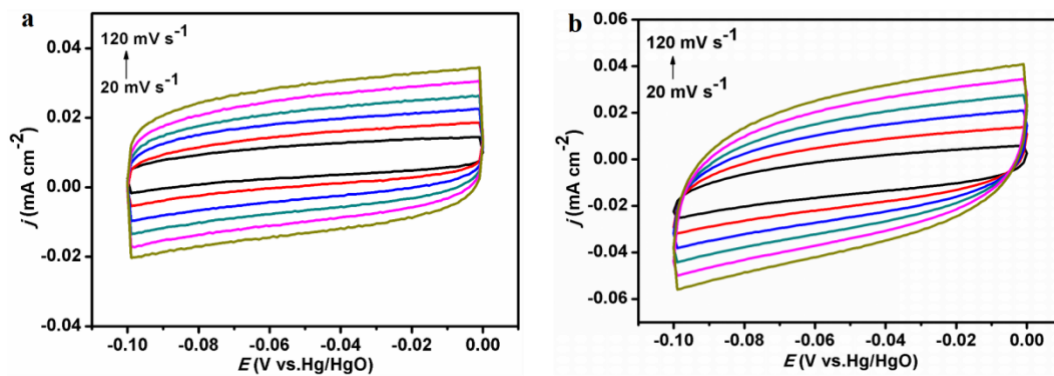


Fig. S7 Cyclic voltammograms in the range of -0.1 to 0 V vs. Hg/HgO with different scan rates of 20, 40, 60, 80, 100 and 120 mV s⁻¹ for (a) **Ag-MOF1** and (b) **Ag-MOF2**.

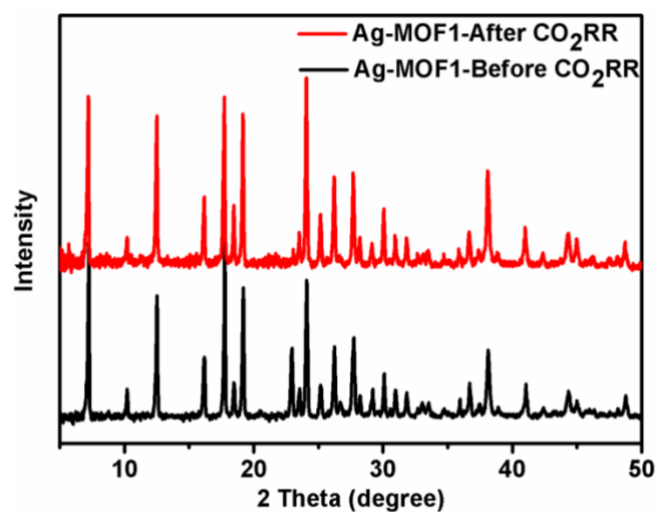


Fig. S8 PXRD patterns of **Ag-MOF1** before and after CO₂RR test.

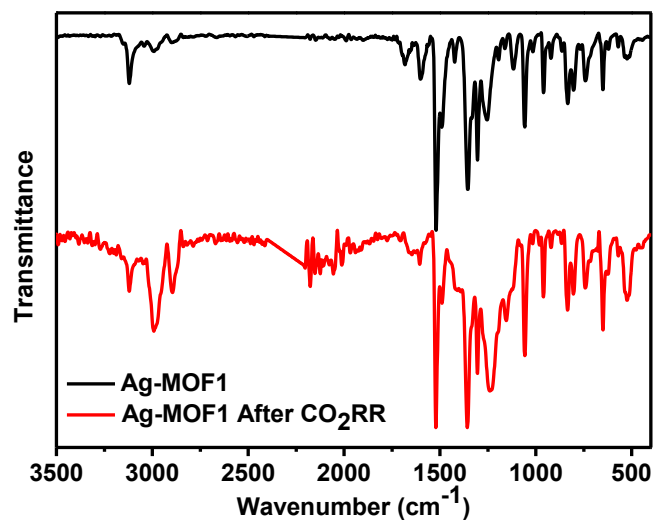


Fig. S9 FT-IR spectra of **Ag-MOF1** before and after CO_2RR test.

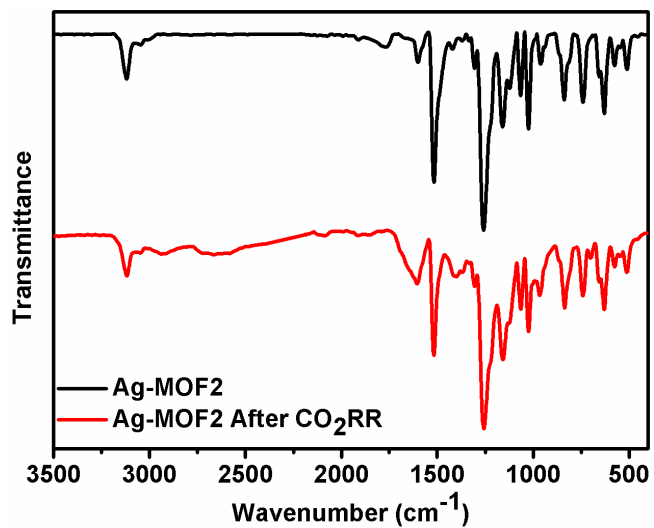


Fig. S10 FT-IR spectra of **Ag-MOF2** before and after CO_2RR test.

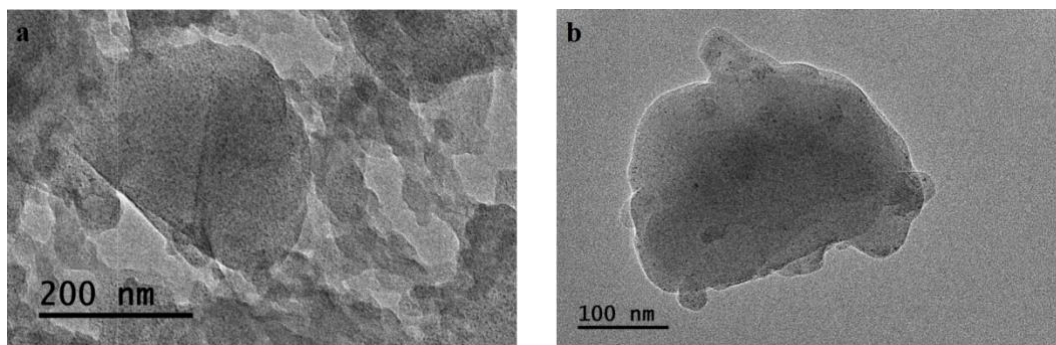


Fig. S11 TEM of (a) **Ag-MOF1** and (b) **Ag-MOF2**.

Table S2. Comparison the selectivity and partial current density of CO production with reported catalysts.

Catalysts	Electrolyte	FE _{CO} (%)	Partial Current Density of CO (mA cm ⁻²)	Ref.
Ag-MOF1	1 M KOH	78.02	28.45	this work
Ag-MOF2	1 M KOH	92.21	29.51	this work
Fe-PMOF	0.5 M KHCO ₃	29.0	4.9	[2]
Ni-PMOF	0.5 M KHCO ₃	19.0	3.2	[2]
Co-PMOF	0.5 M KHCO ₃	99.0	19.5	[2]
[Al ₂ (OH) ₂ (Co(tcpp))]	0.5 M KHCO ₃	76	1.0	[3]
Fe-MOF-525	1 M tbaPF ₆ in CH ₃ CN	60	2.3	[4]
ZIF-8	0.5 M NaCl	65	~3	[5]
PCN-222-Fe	0.5 M KHCO ₃	91.0	1.2	[6]
{Ag ₄₉ Mo ₁₆ }	0.5 M KHCO ₃	44.75	~10	[7]

References

- [1] H. Chen, P. X. Liu, N. Xu, X. Meng, H. N. Wang and Z. Y. Zhou, *Dalton Trans.*, 2016, **45**, 13477-13482.
- [2] Y. R. Wang, Q. Huang, C. T. He, Y. F. Chen, J. Liu, F. C. Shen and Y. Q. Lan, *Nat. Commun.*, 2018, **9**, 4466.
- [3] N. Kornienko, Y. B. Zhao, C. S. Kiley, C. H. Zhu, D. Kim, S. Lin, C. J. Chang, O. M. Yaghi and P. D. Yang, *J. Am. Chem. Soc.*, 2015, **137**, 14129-14135.

- [4] I. Hod, M. D. Sampson, P. Deria, C. P. Kubiak, O. K. Farha and J. T. Hupp, *ACS Catal.*, 2015, **5**, 6302-6309.
- [5] Y. Wang, P. Hou, Z. Wang and P. Kang, *ChemPhysChem*, 2017, **18**, 3142.
- [6] B. X. Dong, S. L. Qian, F. Y. Bu, Y. C. Wu, and Z. W. Li, *ACS Appl. Energy Mater.*, 2018, **1**, 4662-4669.
- [7] S. Q. Li, L. F. Dai, Y. Q. Tian, Y. X. Yi, J. Yan and C. Liu, *Chem. Commun.*, 2023, **59**, 575-578.